Improved lift and drag estimates using adjoint Euler equations

Michael B. Giles*
Oxford University Computing Laboratory, Oxford, OX1 3QD, UK.
Niles A. Pierce†
Division of Biology, California Institute of Technology, Pasadena, CA 91125.

Abstract

This paper demonstrates the use of adjoint error analysis to improve the order of accuracy of integral functionals obtained from CFD calculations. Using second order accurate finite element solutions of the Poisson equation, fourth order accuracy is achieved for two different categories of functional in the presence of both curved boundaries and singularities. Similarly, numerical results for the Euler equations obtained using standard second order accurate approximations demonstrate fourth order accuracy for the integrated pressure in two quasi-1D test cases, and a significant improvement in accuracy in a two-dimensional case. This additional accuracy is achieved at the cost of an adjoint calculation similar to those performed for design optimization.

1 Introduction

In aeronautical CFD, engineers desire very accurate prediction of the lift and drag on aircraft, but they are less concerned with the precise details of the flow field in general, although there is a clear need to understand the qualitative nature of the flow (e.g. is there a bad flow separation?) in order to make design changes which will improve the lift or drag. Similarly, other areas of CFD analysis also have a particular interest in a few key integral quantities, such as total production of nitrous oxides in combustion modeling, or the net seepage of a pollutant into an aquifer when modeling soil contamination.

The objective of this paper is to obtain higher order accuracy for integral functionals (such as the lift and drag) derived from CFD calculations. The key is the solution of the adjoint p.d.e. with inhomogeneous terms appropriate to the functional of interest. We show that it is this solution which relates the error in the original approximation (as measured by the extent to which the approximate solution fails to satisfy the original p.d.e.) to the consequential error in the computed value of the functional. Given an approximation to the adjoint solution, one can then quantify and correct the leading order error term in the functional estimate. The corrected value of the functional is then *superconvergent* in that the remaining error is proportional to the product of the errors in the primal and adjoint solutions.

The analysis is closely related to superconvergence results in the finite element literature [2, 3, 4, 13, 14, 15]. The key distinction is that the adjoint error correction term which we evaluate to obtain superconvergence is zero in a large class of finite element methods, including many which are used for incompressible flow, but not those used most commonly for compressible flow. Thus, these methods automatically produce superconvergent results for any integral functional without requiring the computation of an approximate adjoint solution.

Previous papers by the present authors [9, 16] derived the underlying theory for a limited class of functionals and presented numerical results for the one-dimensional Poisson equation and the quasi-1D Euler equations. The only 2D results were for the Poisson equation on a unit square. In this paper we address a number of issues which are critical to real multi-dimensional applications. The first is the consideration of functionals which are integrals over the boundary of the domain (as in lift and drag integrals) rather than integrals over

*Professor, Member AIAA, giles@comlab.ox.ac.uk, www.comlab.ox.ac.uk
†Senior Postdoctoral Scholar, Member AIAA, niles@mayo.caltech.edu, www.mayo.caltech.edu

the interior of the domain (as in the average temperature of a fluid). The second is consideration of domains with curved boundaries and other more general boundary conditions for which there are truncation errors in the approximation of the boundary conditions. These two features require extensions to the theory presented previously. The third issue, which can be important in multi-dimensional applications, is the presence of singularities in the geometry or solution, such as at the trailing edge of a cusped airfoil. No new theory is required in this case, but the question is whether the presence of a singularity may prevent one from achieving superconvergent results.

We begin the paper by presenting the linear theory and simple examples of its application to the two-dimensional Poisson equation in curved domains. Superconvergent results are achieved even when there is a singularity in the solution. We then present the nonlinear theory and examples of its use with the quasi-1D and 2D Euler equations approximated by standard second order finite volume methods. Unambiguous fourth order accuracy is achieved for the quasi-1D results for both subsonic and shock-free transonic flow. The 2D results show a very significant improvement in the accuracy of the computed functional, but it is not possible to infer the precise order of accuracy.

2 Linear analysis

2.1 Theory without boundary terms

Let u be the solution of the linear differential equation

$$Lu = f,$$

on the domain Ω, subject to homogeneous boundary conditions for which the problem is well-posed when $f \in L_2(\Omega)$. The adjoint differential operator L^* and associated homogeneous boundary conditions are defined by the identity

$$(v, Lu) = (L^*v, u),$$

for all u, v satisfying the respective boundary conditions. Here the notation $(.,.)$ denotes an integral inner product over the domain Ω.

Suppose now that we are concerned with the value of the functional $J = (g, u)$, for a given function $g \in L_2(\Omega)$. An equivalent dual formulation of the problem is to evaluate the functional $J = (v, f)$, where v satisfies the adjoint equation

$$L^*v = g,$$

subject to the homogeneous adjoint boundary conditions. The equivalence of the two forms of the problem follows immediately from the definition of the adjoint operator.

$$(v, f) = (v, Lu) = (L^*v, u) = (g, u).$$

Suppose that u_h and v_h are approximations to u and v, respectively, and satisfy the homogeneous boundary conditions. The subscript h is intended to denote that the approximate solutions are derived from a numerical computation using a grid with average spacing h. When using finite difference or finite volume methods, u_h and v_h might be created by interpolation through computed values at grid nodes. With finite element solutions, one might simply use the finite element solutions themselves, or one could again use interpolation through nodal values and thereby obtain approximate solutions which are smoother than the finite element solutions.

Let the functions f_h and g_h be defined by

$$Lu_h = f_h, \quad L^*v_h = g_h.$$

It is assumed that u_h and v_h are sufficiently smooth that f_h and g_h lie in $L_2(\Omega)$. If u_h and v_h were equal to u and v, then f_h and g_h would be equal to f and g. Thus, the *residual errors* $f_h - f$ and $g_h - g$ are a computable indication of the extent to which u_h and v_h are not the true solutions.

Now, using the definitions and identities given above, we obtain the following expression for the functional:

$$\begin{aligned}
(g, u) &= (g, u_h) - (g_h, u_h - u) + (g_h - g, u_h - u) \\
&= (g, u_h) - (L^*v_h, u_h - u) + (g_h - g, u_h - u) \\
&= (g, u_h) - (v_h, L(u_h - u)) + (g_h - g, u_h - u) \\
&= (g, u_h) - (v_h, f_h - f) + (g_h - g, u_h - u).
\end{aligned}$$

The first term in the final expression is the value of the functional obtained from the approximate solution u_h. The second term is an inner product of the residual error $f_h - f$ and the approximate adjoint solution v_h. The adjoint solution gives the weighting of the contribution of the local residual error to the overall error in the computed functional. Therefore, by evaluating and subtracting this adjoint error term we obtain a more accurate value for the functional.

The third term is the remaining error after making the adjoint correction. If $g_h - g$ is of the same order of magnitude as $v_h - v$ then, using L_2 norms, the remaining error has a bound which is proportional to the product $\|u_h - u\| \, \|v_h - v\|$, and thus the corrected functional value

is superconvergent. If the solution errors $u_h - u$ and $v_h - v$ are both $O(h^p)$ then the error in the functional is $O(h^{2p})$. Furthermore, the remaining error term can be expressed as $(g_h - g, L^{-1}(f_h - f))$ and so has the computable *a posteriori* error bound $\|L^{-1}\| \, \|f_h - f\| \, \|g_h - g\|$.

2.2 First example

In a previous paper [9], we demonstrated the effectiveness of the error correction technique for the two-dimensional Poisson equation

$$\frac{\partial^2 U}{\partial X^2} + \frac{\partial^2 U}{\partial Y^2} = F(X, Y)$$

on a unit square domain subject to homogeneous Dirichlet boundary conditions. Using a second order accurate finite element method with bilinear test and trial functions, fourth order accuracy was achieved for the functional (G, U) for the particular case in which

$$F = X(1-X)\,Y(1-Y), \quad G = \sin(\pi X)\,\sin(\pi Y).$$

To show that superconvergence can also be achieved on domains with curved boundaries, we use conformal mapping to transform this same problem into a mathematically equivalent form. Defining the complex variables Z and z as

$$Z \equiv X + iY, \quad z \equiv x + iy,$$

the mapping

$$z = (Z + 3 + i)^2$$

maps the unit square onto the 'warped square' shown in Figure 1. $u(x, y) \equiv U(X, Y)$ is then the solution of the transformed p.d.e.

$$\frac{\partial^2 u}{\partial x^2} + \frac{\partial^2 u}{\partial y^2} = f(x, y),$$

with

$$f(x, y) = F(X, Y) \left| \frac{dZ}{dz} \right|^2 .$$

Similarly, the transformed functional is (g, u) where

$$g(x, y) = G(X, Y) \left| \frac{dZ}{dz} \right|^2 .$$

The exact value of the functional can be determined analytically. Numerical results have been obtained using a Galerkin finite element method with piecewise bilinear elements on the curved mesh in the z-plane. Standard finite element error analysis reveals that both the solution error for the primal problem and the error in the computed functional using the finite element solution are $O(h^2)$. However, by bi-cubic spline interpolation of the nodal values and the grid coordinates at the nodal points, one can reconstruct in parametric form an improved approximate solution $u_h(x, y)$ with an error which is $O(h^2)$ in the H^2 Sobolev norm and hence has a residual error which is also $O(h^2)$. Using a similarly reconstructed approximate adjoint solution $v_h(x, y)$, one can then compute the adjoint error correction term resulting in a corrected functional whose accuracy is $O(h^4)$. All inner product integrals are approximated by 3×3 Gaussian quadrature on each quadrilateral cell to ensure that the numerical quadrature errors are of a higher order.

Figure 2 shows the error in the computed value for the functional, before and after the adjoint correction, together with the bound for the remaining error. The ordinate is the logarithm of the number of cells in each dimension. Lines of slope -2 and -4 passing through the final data points are superimposed to show that the base error in the functional is clearly second order whereas the error in the corrected value of the functional is fourth order.

Note also that an error level of 10^{-8} is achieved with a grid of 16×16 when using the adjoint error correction, whereas it requires a grid of 256×256 without the error correction. Thus, the computational savings are enormous and more than justify the cost of the adjoint calculation.

2.3 Theory with boundary terms

We now extend the theory to include inhomogeneous boundary conditions for the primal and dual problems, and boundary integrals in their output functionals.

Let u be the solution of the linear differential equation

$$Lu = f,$$

in the domain Ω, subject to the linear boundary conditions

$$Bu = e,$$

on the boundary $\partial\Omega$. In general, the dimension of the operator B will be different on different sections of the boundary (e.g. inflow and outflow sections for the convection p.d.e.).

The output functional of interest is taken to be

$$J = (g, u) + (h, Cu)_{\partial\Omega},$$

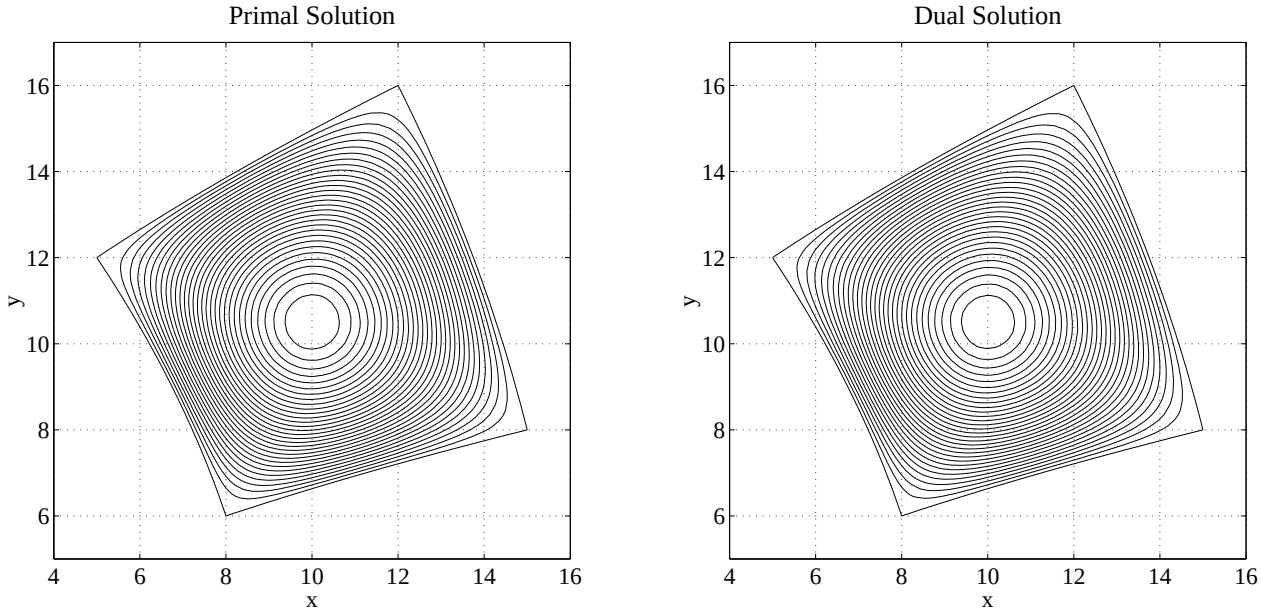

Figure 1: The reconstructed primal and dual solutions for a 2D Poisson problem on a warped square.

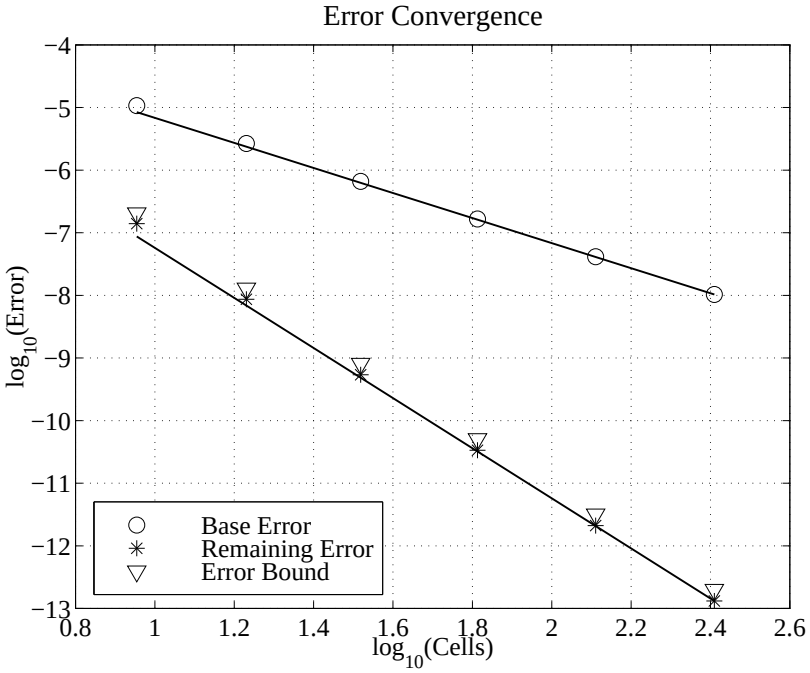

Figure 2: Error convergence of a bulk functional for a 2D Poisson problem on a warped square.

where $(.,.)_{\partial\Omega}$ represents an integral inner product over the boundary $\partial\Omega$. The boundary operator C may be algebraic (e.g. $Cu \equiv u$) or differential (e.g. $Cu \equiv \frac{\partial u}{\partial n}$), but must have the same dimension as the adjoint boundary condition operator B^* to be defined shortly. Note that the components of h may be set to zero if the functional does not have a boundary integral contribution.

The corresponding linear adjoint problem is

$$L^* v = g,$$

in Ω, subject to the boundary conditions

$$B^* v = h,$$

on the boundary $\partial\Omega$. The fundamental identity defining L^*, B^* and the boundary operator C^* is

$$(L^* v, u) + (B^* v, Cu)_{\partial\Omega} = (v, Lu) + (C^* v, Bu)_{\partial\Omega},$$

for all u, v. This identity is obtained by integration by parts, and in a previous paper we describe the construction of the appropriate adjoint operators for the linearized Euler and Navier-Stokes equations [7].

Using the adjoint identity, one immediately obtains the equivalent dual form of the output functional,

$$J = (v, f) + (C^* v, e)_{\partial\Omega}.$$

Given approximate solutions u_h, v_h we define e_h, f_h, g_h, h_h by

$$\begin{aligned} Lu_h &= f_h, \quad & L^* v_h &= g_h, \\ Bu_h &= e_h, \quad & B^* v_h &= h_h, \end{aligned}$$

and hence obtain

$$\begin{aligned} &(g, u) + (h, Cu)_{\partial\Omega} \\ &\quad = (g, u_h) + (h, Cu_h)_{\partial\Omega} \\ &\qquad -(g_h, u_h - u) - (h_h, C(u_h - u))_{\partial\Omega} \\ &\qquad +(g_h - g, u_h - u) + (h_h - h, C(u_h - u))_{\partial\Omega} \\ &\quad = (g, u_h) + (h, Cu_h)_{\partial\Omega} \\ &\qquad -(L^* v_h, u_h - u) - (B^* v_h, C(u_h - u))_{\partial\Omega} \\ &\qquad +(g_h - g, u_h - u) + (h_h - h, C(u_h - u))_{\partial\Omega} \\ &\quad = (g, u_h) + (h, Cu_h)_{\partial\Omega} \\ &\qquad -(v_h, L(u_h - u)) - (C^* v_h, B(u_h - u))_{\partial\Omega} \\ &\qquad +(g_h - g, u_h - u) + (h_h - h, C(u_h - u))_{\partial\Omega} \\ &\quad = (g, u_h) + (h, Cu_h)_{\partial\Omega} \\ &\qquad -(v_h, f_h - f) - (C^* v_h, e_h - e)_{\partial\Omega} \\ &\qquad +(g_h - g, u_h - u) + (h_h - h, C(u_h - u))_{\partial\Omega}. \end{aligned}$$

In the final result, the first line is the functional based on the approximate solution u_h. The second line is the adjoint correction term which now includes a term related to the extent to which the primal solution does not correctly satisfy the boundary conditions. The third line is the remaining error for which an *a posteriori* error bound can again be found.

2.4 Second example

In addition to curved boundaries, it is also interesting to investigate the influence of geometric singularities in the domain, such as the cusp at the trailing edge of an airfoil.

Using the same conformal mapping approach as above, we define the domain in the Z-plane to be the region between two circles centered at $(X, Y) = (-0.1, 0)$ with radii of $R_1 = 1.1$ and $R_2 = 3.0$. Application of the Joukowski mapping

$$z = Z + \frac{1}{Z},$$

then produces a computational domain between a cusped airfoil ($\partial\Omega_{z1}$) and a smooth outer boundary ($\partial\Omega_{z2}$).

Using cylindrical coordinates R, θ defined by

$$X + 0.1 = R\cos\theta, \quad Y = R\sin\theta,$$

the function

$$U(X, Y) = \frac{R^2 - R_1^2}{R}\sin\theta,$$

is a solution of the Laplace equation subject to the boundary conditions $U = 0$ on the inner circle, and

$$U = \frac{R_2^2 - R_1^2}{R_2}\sin\theta,$$

on the outer cylinder.

In the z-plane, the function $u(x, y) = U(X, Y)$ is the solution of the Laplace equation

$$\frac{\partial^2 u}{\partial x^2} + \frac{\partial^2 u}{\partial y^2} = 0,$$

subject to $u = 0$ on the airfoil, and the appropriate Dirichlet boundary conditions on the far-field boundary. As illustrated in Figure 3, this solution corresponds to the stream function for incompressible inviscid flow around the airfoil, with zero circulation.

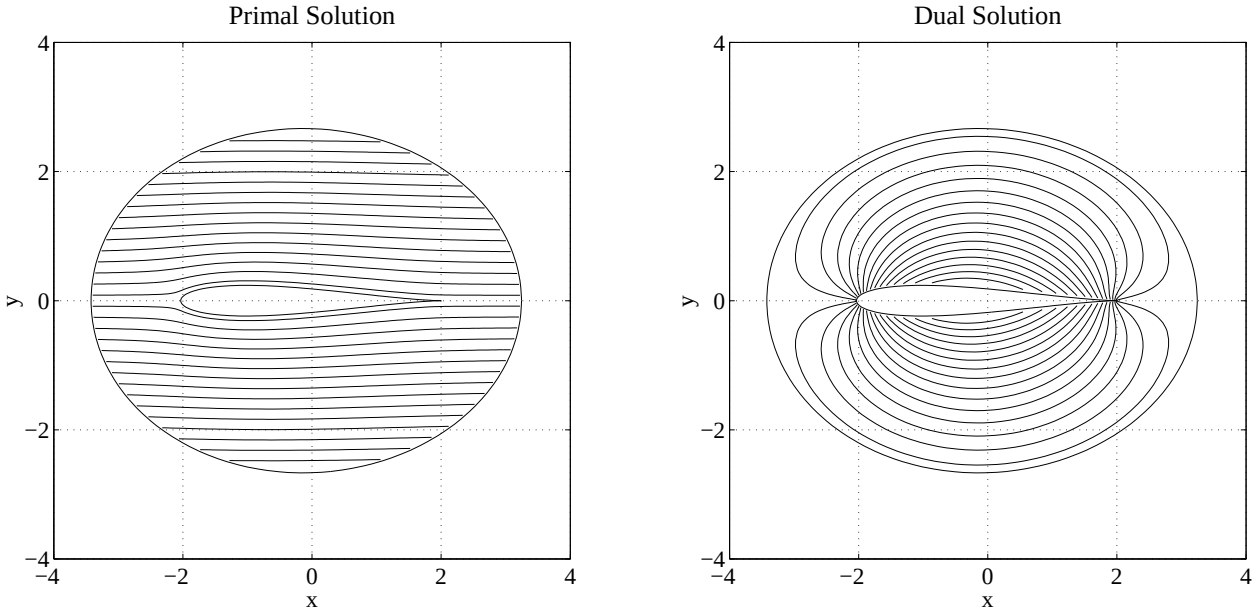

Figure 3: The reconstructed primal and dual solutions for a 2D Laplace problem around a Joukowski airfoil.

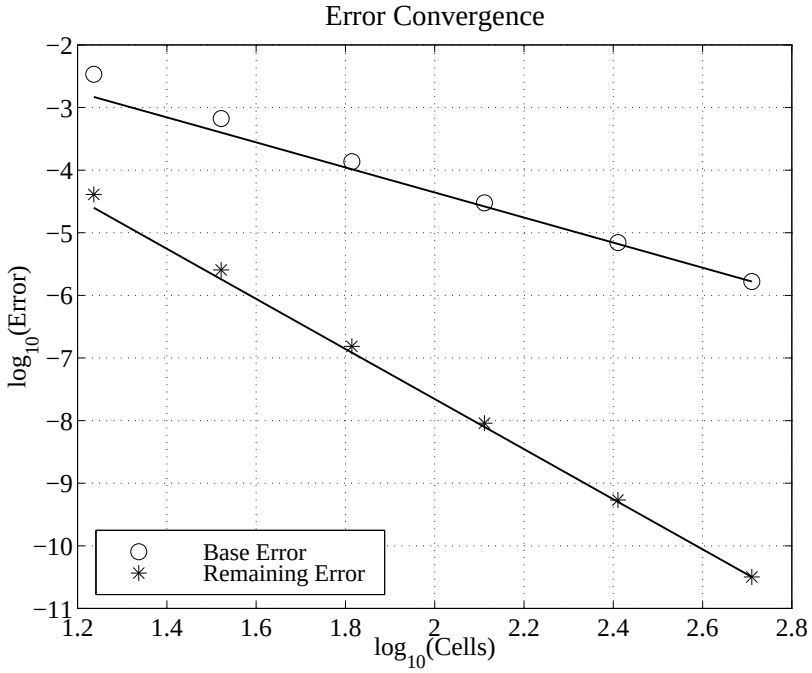

Figure 4: Error convergence of a boundary functional for a 2D Laplace problem around a Joukowski airfoil.

The boundary functional in the Z-plane is defined to be

$$\int_0^{2\pi} H(\theta)\ \frac{\partial U}{\partial n}\bigg|_{R=R_1} d\theta,$$

where

$$H = \frac{\sin\theta}{R_1},$$

and its value can be obtained analytically. When mapped into the z-plane, the corresponding expression for the functional is

$$\left(H, \frac{\partial u}{\partial n}\right)_{\partial\Omega_{z1}},$$

and hence the dual problem is the Laplace equation subject to the inhomogeneous Dirichlet condition $v = H$ on the airfoil surface and $v = 0$ on the far-field boundary.

Figure 4 shows the numerical results obtained using the same Galerkin finite element method, bi-cubic spline interpolation and 2×2 Gaussian quadrature, owing to memory constraints resulting from a larger computational mesh. The solution is splined periodically around the airfoil, including on the surface where there is a cusp in the geometry. The errors produced by this treatment of the geometric singularity at the trailing edge converge faster then the second order accuracy of the baseline finite element method.

Again the superimposed lines of slope -2 and -4 show that the base solution is second order accurate whereas the corrected value for the functional is fourth order accurate.

3 Nonlinear theory

The nonlinear theory in the absence of boundary integrals in the functional and errors in approximating the boundary conditions has been presented previously [9, 16], and so we now proceed directly to the theory including boundary effects which is presented here for the first time.

Let u be the solution of the nonlinear differential equation

$$N(u) = 0,$$

in the domain Ω, subject to the nonlinear boundary conditions

$$D(u) = 0,$$

on the boundary $\partial\Omega$.

The linear differential operators L_u and B_u are defined to be the Fréchet derivatives of N and D, respectively,

$$L_u\,\tilde{u} \equiv \lim_{\epsilon\to 0} \frac{N(u+\epsilon\tilde{u}) - N(u)}{\epsilon},$$
$$B_u\,\tilde{u} \equiv \lim_{\epsilon\to 0} \frac{D(u+\epsilon\tilde{u}) - D(u)}{\epsilon}.$$

It is assumed that the nonlinear functional of interest, $J(u)$, has a Fréchet derivative of the following form,

$$\lim_{\epsilon\to 0} \frac{J(u+\epsilon\tilde{u}) - J(u)}{\epsilon} = (g(u), \tilde{u}) + (h, C_u\tilde{u})_{\partial\Omega}.$$

Here the dimension of the operator C_u (which may be differential) is required to equal the dimension of the adjoint boundary operator B_u^*, to be defined shortly.

The corresponding linear adjoint problem is

$$L_u^* v = g(u)$$

in Ω, subject to the boundary conditions

$$B_u^* v = h$$

on the boundary $\partial\Omega$. The identity defining L_u^*, B_u^* and the boundary operator C_u^* is

$$(L_u^* v, \tilde{u}) + (B_u^* v, C_u\tilde{u})_{\partial\Omega} = (v, L_u\tilde{u}) + (C_u^* v, B_u\tilde{u})_{\partial\Omega},$$

for all $\tilde{u}, v$.

We now consider approximate solutions u_h, v_h and define g_h, h_h by

$$L_{u_h}^* v_h = g_h, \qquad B_{u_h}^* v_h = h_h$$

Note the use of the Fréchet derivatives based on u_h which is known, instead of those based on u which is not known.

The analysis also requires averaged Fréchet derivatives defined by

$$\begin{aligned}
\overline{L}_{(u,u_h)} &= \int_0^1 L|_{u+\theta(u_h-u)}\, d\theta,\\
\overline{B}_{(u,u_h)} &= \int_0^1 B|_{u+\theta(u_h-u)}\, d\theta,\\
\overline{C}_{(u,u_h)} &= \int_0^1 C|_{u+\theta(u_h-u)}\, d\theta,\\
\overline{g}(u,u_h) &= \int_0^1 g(u+\theta(u_h-u))\, d\theta,
\end{aligned}$$

so that

$$\begin{aligned}
N(u_h) - N(u) &= \int_0^1 \frac{\partial}{\partial\theta} N(u+\theta(u_h-u))\, d\theta\\
&= \overline{L}_{(u,u_h)}\,(u_h-u),
\end{aligned}$$

and similarly

$$\begin{aligned} D(u_h)-D(u) &= \overline{B}_{(u,u_h)}\,(u_h-u), \\ J(u_h)-J(u) &= (\overline{g}(u,u_h),u_h-u) \\ &\quad +(h,\overline{C}_{(u,u_h)}(u_h-u))_{\partial\Omega}. \end{aligned}$$

We now obtain the following:

$$\begin{aligned} & J(u_h)-J(u) \\ &= (\overline{g}(u,u_h),u_h-u)+(h,\overline{C}_{(u,u_h)}(u_h-u))_{\partial\Omega} \\ &= (g_h,u_h-u)+(h_h,C_{u_h}(u_h-u))_{\partial\Omega} \\ &\quad -(g_h-\overline{g}(u,u_h),u_h-u) \\ &\quad -(h,(C_{u_h}-\overline{C}_{(u,u_h)})(u_h-u))_{\partial\Omega} \\ &\quad -(h_h-h,C_{u_h}(u_h-u))_{\partial\Omega} \\ &= (L^*_{u_h}v_h,u_h-u)+(B^*_{u_h}v_h,C_{u_h}(u_h-u))_{\partial\Omega} \\ &\quad -(g_h-\overline{g}(u,u_h),u_h-u) \\ &\quad -(h,(C_{u_h}-\overline{C}_{(u,u_h)})(u_h-u))_{\partial\Omega} \\ &\quad -(h_h-h,C_{u_h}(u_h-u))_{\partial\Omega} \\ &= (v_h,L_{u_h}(u_h-u))+(C^*_{u_h}v_h,B_{u_h}(u_h-u))_{\partial\Omega} \\ &\quad -(g_h-\overline{g}(u,u_h),u_h-u) \\ &\quad -(h,(C_{u_h}-\overline{C}_{(u,u_h)})(u_h-u))_{\partial\Omega} \\ &\quad -(h_h-h,C_{u_h}(u_h-u))_{\partial\Omega} \\ &= (v_h,\overline{L}_{(u,u_h)}(u_h-u))+(C^*_{u_h}v_h,\overline{B}_{(u,u_h)}(u_h-u))_{\partial\Omega} \\ &\quad -(g_h-\overline{g}(u,u_h),u_h-u) \\ &\quad -(h,(C_{u_h}-\overline{C}_{(u,u_h)})(u_h-u))_{\partial\Omega} \\ &\quad -(h_h-h,C_{u_h}(u_h-u))_{\partial\Omega} \\ &\quad +(v_h,(L_{u_h}-\overline{L}_{(u,u_h)})(u_h-u)) \\ &\quad +(C^*_{u_h}v_h,(B_{u_h}-\overline{B}_{(u,u_h)})(u_h-u))_{\partial\Omega} \\ &= (v_h,N(u_h))+(C^*_{u_h}v_h,D(u_h))_{\partial\Omega} \\ &\quad -(g_h-\overline{g}(u,u_h),u_h-u) \\ &\quad -(h,(C_{u_h}-\overline{C}_{(u,u_h)})(u_h-u))_{\partial\Omega} \\ &\quad -(h_h-h,C_{u_h}(u_h-u))_{\partial\Omega} \\ &\quad +(v_h,(L_{u_h}-\overline{L}_{(u,u_h)})(u_h-u)) \\ &\quad +(C^*_{u_h}v_h,(B_{u_h}-\overline{B}_{(u,u_h)})(u_h-u))_{\partial\Omega}. \end{aligned}$$

In the final result, the first line is the adjoint correction term taking into account residual errors in approximating both the p.d.e. and the boundary conditions. The other lines are the remaining errors, which include the consequences of nonlinearity in L, B, C and g as well as residual errors in approximating the adjoint problem.

If the solution errors for the nonlinear primal problem and the linear adjoint problem are of the same order, and they are both sufficiently smooth that the corresponding residual errors are also of the same order, then the order of accuracy of the functional approximation after making the adjoint correction is twice the order of the primal and adjoint solutions. However, rigorous *a priori* and *a posteriori* analysis of the remaining errors is much harder than in the linear case [16] and practical *a posteriori* error bounds have yet to be obtained for the quasi-1D and 2D Euler equations.

4 Quasi-1D Euler equations

The steady quasi-1D Euler equations for the flow of an ideal compressible fluid in a variable area duct are

$$\frac{d}{dx}(AF)-\frac{dA}{dx}\,P=0,$$

where $A(x)$ is the cross-sectional area of the duct and U, F and P are defined as

$$U=\begin{pmatrix}\rho\\ \rho q\\ \rho E\end{pmatrix},\qquad F=\begin{pmatrix}\rho q\\ \rho q^2+p\\ \rho q H\end{pmatrix},\qquad P=\begin{pmatrix}0\\ p\\ 0\end{pmatrix}.$$

Here ρ is the density, q is the velocity, p is the pressure, E is the total energy and H is the stagnation enthalpy. The system is closed by the equation of state for an ideal gas. The functional of interest is the 'lift'

$$J=\int p\;dx.$$

The equations are approximated using a standard second order finite volume method with characteristic smoothing on a uniform computational grid. The linear adjoint problem is approximated by the so-called 'continuous' method, which involves linearizing the nonlinear flow equations, constructing the analytic adjoint equations, and then forming a discrete approximation to these on the same uniform grid as the flow solution [1, 11]. The alternative 'discrete' approach, in which one takes the discretized nonlinear flow equations, linearizes them and then uses the transpose of the linear matrix as the discrete adjoint operator [5], is employed for the two-dimensional calculation presented later in the paper. Previous research has shown that both approaches produce consistent approximations to the analytic adjoint solution, which has been determined in closed form for the quasi-1D Euler equations [8].

The approximate solution $u_h(x)$ is constructed from the discrete flow solution by cubic spline interpolation of the nodal values of the three components of the state

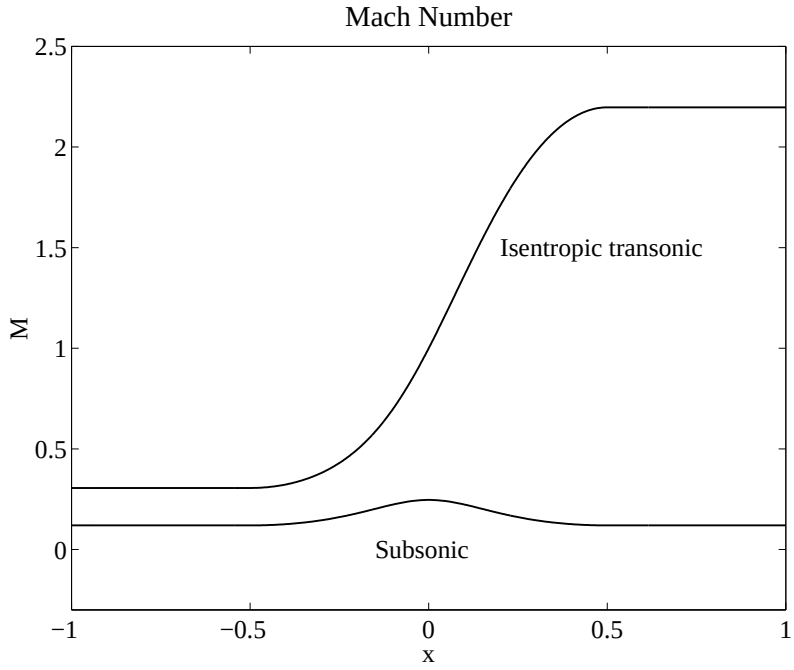

Figure 5: Mach number distributions for quasi-1D Euler equation test cases.

vector U. Similarly, the approximate adjoint solution $v_h(x)$ is obtained by cubic spline interpolation of the nodal values of the three components of the discrete adjoint solution. The integrals which form the base value for the functional and the adjoint correction are approximated by 3-point Gaussian quadrature.

4.1 Subsonic flow

The first case is smooth subsonic flow in a converging-diverging duct corresponding to the Mach number distribution depicted in Figure 5. Figure 6 shows the error convergence for the computed functional. The superimposed lines of slope -2 and -4 show that the base error is second order whereas the error in the corrected functional is fourth order. This is in agreement with an *a priori* error analysis [16] which proves that $u_h - u$, $v_h - v$ and their first derivatives are all $O(h^2)$ for the particular finite volume scheme which is used, and hence the error in the corrected functional is $O(h^4)$.

4.2 Isentropic transonic flow

Figure 7 shows the error convergence for a transonic flow in a converging-diverging duct corresponding to the Mach number distribution of Figure 5. The flow is subsonic at the inflow boundary and upstream of the throat (located at $x = 0$), and supersonic downstream of the throat and at the outflow boundary. Again the results show that the base error is second order while the remaining error after the adjoint correction is fourth order, even though there is logarithmic singularity in the adjoint solution at the throat [8].

5 2D Euler equations

The nonlinear steady-state Euler equations in conservation form are

$$\frac{\partial}{\partial x} F_x(U) + \frac{\partial}{\partial y} F_y(U) = 0,$$

where U is the vector of conserved variables and $F_x(U)$ and $F_y(U)$ are the nonlinear flux functions

$$U = \begin{pmatrix} \rho \\ \rho q_x \\ \rho q_y \\ \rho E \end{pmatrix}, \quad F_x = \begin{pmatrix} \rho q_x \\ \rho q_x^2 + p \\ \rho q_x q_y \\ \rho q_x H \end{pmatrix}, \quad F_y = \begin{pmatrix} \rho q_y \\ \rho q_x q_y \\ \rho q_y^2 + p \\ \rho q_y H \end{pmatrix}.$$

The preceding test cases dealt with many of the theoretical and practical issues that are likely to arise in CFD calculations, including curved boundaries, geometric singularities and nonlinear systems. To take the next step, the present example demonstrates error correction for subsonic inviscid compressible flow through a

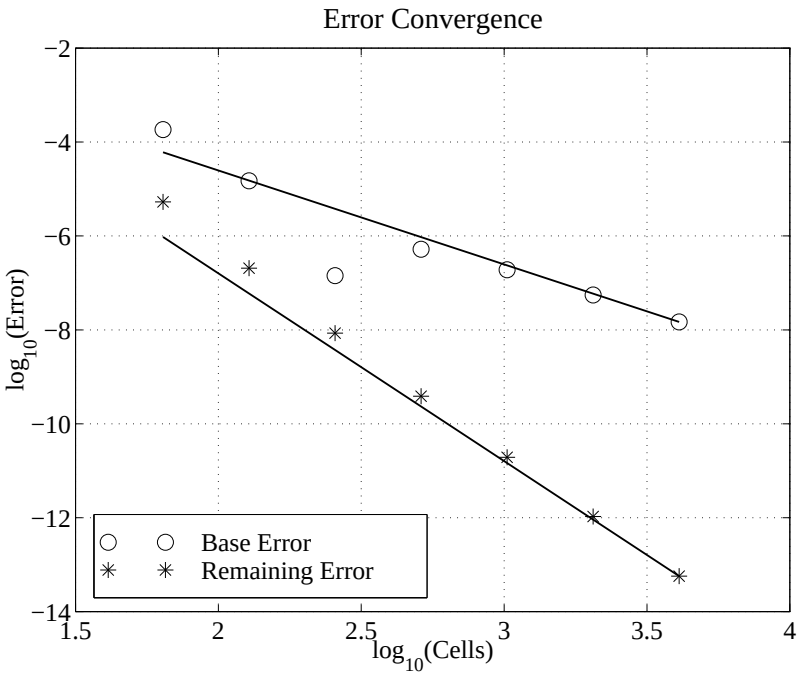

Figure 6: Error convergence for quasi-1D subsonic flow.

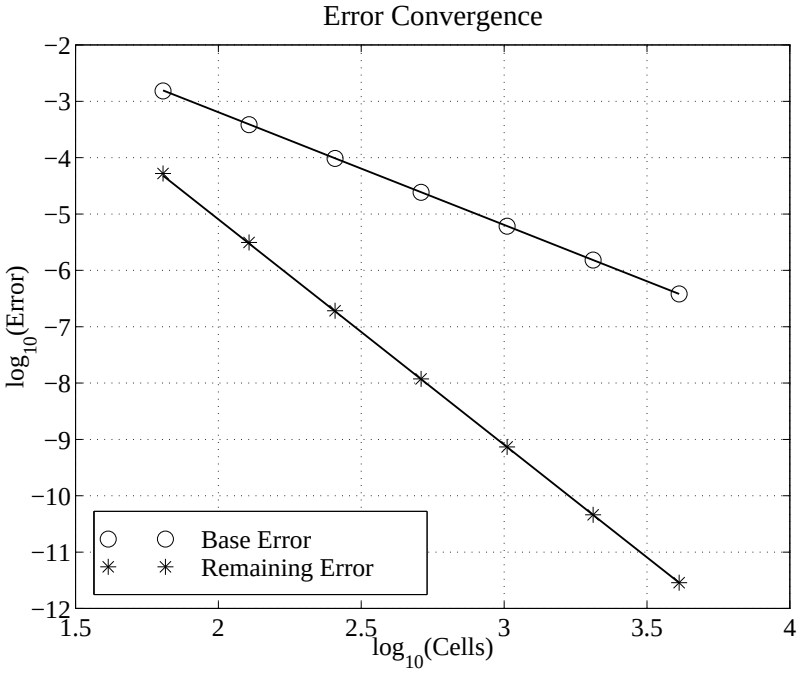

Figure 7: Error convergence for quasi-1D shock-free transonic flow.

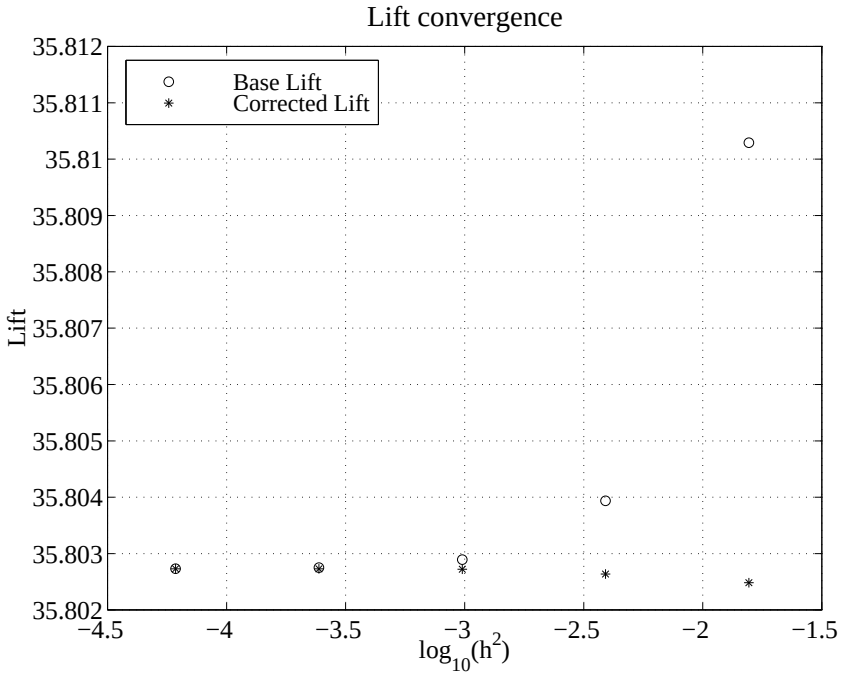

Figure 8: Lift convergence for subsonic flow in a 2D nozzle.

smooth converging-diverging duct that has a 10% constriction at the throat relative to the inlet and outlet areas. To assist in the validation of the code, the functional is chosen to mimic the 'lift' of the quasi-1D cases,

$$J = \tfrac{1}{2} \int (p_{\text{top}} + p_{\text{bottom}})\, dx.$$

The flow solution is computed with a standard second order finite volume discretization on a structured mesh composed of quadrilateral cells. The adjoint solution is obtained using the previously described 'discrete' approach. As before, bi-cubic splining of the nodal values and mesh coordinates is used to reconstruct the flow and adjoint solutions. Analytic boundary conditions are enforced during the reconstruction at solid as well as inflow and outflow boundaries so that the boundary terms in the error correction formulation vanish. These boundary errors are propagated to the interior of the domain through the reconstruction, so that they are accounted for in the bulk correction term computed with 3×3 Gaussian quadrature on each mesh cell.

Figure 8 demonstrates that the error correction approach provides a substantial improvement in the accuracy of the functional estimate relative to the baseline lift value. However, since the analytic solution to this problem is not available, it is not possible to determine the order of accuracy as for the previous test cases.

6 Conclusions

In this paper we have presented a method of doubling the order of accuracy of integral quantities derived from CFD calculations. Doing so requires a solution of the adjoint flow equations, which are the same equations used in the optimal aerodynamic design approach of Jameson [10, 11]. Because of the importance of design, many adjoint solvers are currently being developed for the Euler and Reynolds-averaged Navier-Stokes equations [1, 5, 12], facilitating rapid exploitation of the error correction ideas described in this paper.

The theory has been fully developed for both linear and nonlinear p.d.e.'s, and this paper presents for the first time the extensions required to treat boundary integral functionals and truncation errors in the numerical approximation of boundary conditions.

The numerical results for the 2D Poisson and Laplace equations confirm the ability of the error correction to give superconvergence for domains with curved boundaries and even singularities in the geometry and solution, provided there is adequate grid resolution. The results for the quasi-1D Euler equations also show an unambiguous doubling of the order of accuracy for the integrated pressure, confirming that the theory correctly treats nonlinear problems. Thus, these model problems test all of the components of the theory needed for real engineering applications.

The numerical results for the 2D Euler equations are very preliminary in nature. They show a quite significant improvement in the accuracy of the functional but it is not possible to infer the precise order of accuracy of the corrected functional. Also, the test case is very simple, involving a converging-diverging duct with a very mild area contraction. Future work will address much more challenging problems, such as the flow over airfoils and wings.

There are two other issues to be addressed in future research. The current work involves cubic spline interpolation of CFD data on structured grids. On unstructured grids, the construction of a smooth interpolation is a much more difficult task. The use of unstructured grids also introduces the whole topic of optimal grid adaptation [4, 14]. The magnitude of the adjoint error correction term $(v_h, f_h - f)$ can be reduced by adapting the grid in the regions in which the product $v_h^T(f_h - f)$ is largest. Alternatively, if grid adaptation is to be used in conjunction with adjoint error correction then the remaining error is perhaps best minimized by adapting the grid where the residual errors $f_h - f$ and $g_h - g$ are largest.

7 Acknowledgments

Funding for this work was provided by EPSRC under research grant GR/K91149.

References

[1] W.K. Anderson and V. Venkatakrishnan. Aerodynamic design optimization on unstructured grids with a continuous adjoint formulation. AIAA Paper 97-0643, 1997.

[2] I. Babuška and A. Miller. The post-processing approach in the finite element method – Part 1: calculation of displacements, stresses and other higher derivatives of the displacements. *Intern. J. Numer. Methods Engrg.*, 20:1085–1109, 1984.

[3] I. Babuška and A. Miller. The post-processing approach in the finite element method – part 2: the calculation of stress intensity factors. *Intern. J. Numer. Methods Engrg.*, 20:1111–1129, 1984.

[4] R. Becker and R. Rannacher. Weighted a posteriori error control in finite element methods. Technical report, Universitat Heidelberg, 1996. Preprint No. 96-1.

[5] J. Elliott and J. Peraire. Practical 3D aerodynamic design and optimization using unstructured meshes. *AIAA J.*, 35(9):1479–1485, 1997.

[6] M.B. Giles. Analysis of the accuracy of shock-capturing in the steady quasi-1D Euler equations. *Comput. Fluid Dynamics J.*, 5(2):247–258, 1996.

[7] M.B. Giles and N.A. Pierce. Adjoint equations in CFD: duality, boundary conditions and solution behaviour. AIAA Paper 97-1850, 1997.

[8] M.B. Giles and N.A. Pierce. On the properties of solutions of the adjoint Euler equations. In M.J. Baines, editor, *Numerical Methods for Fluid Dynamics VI*, 1998.

[9] M.B. Giles and N.A. Pierce. Superconvergent lift estimates using the adjoint Euler equations. In *Proceedings of Third Asian CFD Conference*, 1998.

[10] A. Jameson. Aerodynamic design via control theory. *J. Sci. Comput.*, 3:233–260, 1988.

[11] A. Jameson. Optimum aerodynamic design using control theory. *Comput. Fluid Dynam. Rev.*, pages 495–528, 1995.

[12] A. Jameson, N.A. Pierce, and L. Martinelli. Optimum aerodynamic design using the Navier–Stokes equations. AIAA Paper 97-0101, 1997.

[13] P. Monk and E. Süli. The adaptive computation of far field patterns by *a posteriori* error estimation of linear functionals. Technical Report NA98/02, Oxford University Computing Laboratory, 1998. To appear in SIAM J. Num. Anal.

[14] M. Paraschivoiu, J. Peraire, and A. Patera. A posteriori finite element bounds for linear-functional outputs of elliptic partial differential equations. *Comput. Methods Appl. Mech. Engrg.*, 150(1-4):289–312, 1997.

[15] J. Peraire and A.T. Patera. Bounds for linear-functional outputs of coercive partial differential equations: local indicators and adaptive refinement. In P. Ladeveze and J.T. Oden, editors, *New Advances in Adaptive Computational Methods in Mechanics*. Elsevier, 1997.

[16] N.A. Pierce and M.B. Giles. Adjoint recovery of superconvergent functionals from approximate solutions of partial differential equations. Technical Report NA98/18, Oxford University Computing Laboratory, 1998.